Journal of Engineering and Applied Science Vol. 4, No. 1, pp. 86–97, June 2020

Journal of Engineering and Applied Science

Contents are available at www.jeas.ruet.ac.bd

Dynamic Behaviour of Ballasted Railway Track Foundation under Various Conditions of the Train-Track-Ground System

Md. Abu Sayeed

Department of Civil Engineering, Rajshahi University of Engineering & Technology
Rajshahi-6204, Bangladesh

ARTICLE INFORMATION

Received date: 30 Jan 2020
Revised date: 20 May 2020
Accepted date: 24 Jun 2020

Keywords

Ballasted railway track
Finite element model
High-speed trains
Subgrade stiffness
Wheel spacing

ABSTRACT

Nowadays, the competition among different public transportation in terms of speed, safety, comfortability, carrying capacity, and cost has significantly increased the demand for faster and heavier trains. This demand indicates probable pressure to build railway tracks appropriate for high-speed trains (HSTs) and heavy wheel loads (HWLs) and they are generally responsible for strong vibrations in the train-track-ground system. They raise the danger of track damages and train derailment. Hence, an investigation into the impact of various parameters that affect the track performance is essential. This study is vital for railway geotechnical engineers to reach an optimum plan for both the railway track design and lifetime maintenance. In this paper, sophisticated three-dimensional finite element modelling has been developed to investigate the impact of various parameters including, train speed, track subgrade thickness, loading amplitude and train geometry on the dynamic responses of the train-track-ground system. The outcomes are critically analyzed and discussed.

1. Introduction

The development of high-speed train (HST) networks is accelerating in many countries of the world as a justifiable solution to the growing demand for faster transportation. For example, the Japan Railways (JR) group has built the Shinkansen (Japanese bullet train) network for trains running at a speed of 320 km/h. On 21 April 2015, the Japanese bullet train (L0 series) set a world speed record of 603 km/h (375 mph) using the magnetic levitation (maglev) technology. Instead, China has the world's largest HST network, which is about 32,200 km long designed for train speeds of 250–350 km/h, and the Chinese railway authority expects that train speed in China will increase up to 600 km/h shortly.

*Corresponding authors: Department of Civil Engineering, Rajshahi University of Engineering & Technology, Rajshahi-6204, Bangladesh
E-mail address: sayeed.ce00@gmail.com (Md. Abu Sayeed)

If train speed and loading amplitude continue to increase, the intensity of the vibration at the train-track-ground system becomes even greater. Because of significant amplification of vibration, new challenges, and difficulties related to track performance arise. Moreover, high-speed trains often produce remarkably large vibrations, especially at the critical speed [1]. The critical speed of the train-track-ground system is the train speed at which the dynamic response of the railway track and surrounding ground are extremely intense and the resonance causes huge vibrations [2, 3]. The raise in vibrations is not only a probable source of a harmful environmental effect, but also raises the danger of several train operation issues. The train operation issues include the deformation or deterioration of track foundation, railway fatigue failure, train safety, and disruption of train's power supply [4].

Problems related to soil vibration due to the dynamic response of moving loads on a surface of an elastic medium have been theoretically studied in the last century [5]. Instead, the failure to operate the X-2000 passenger HST at the Ledsgard site brought up the problem of the impact of train moving loads to the attention of geotechnical engineers. Afterward, various methods including analytical approaches [6], finite element methods (FEM) [7, 8], boundary element models (BEM) [9], and 2.5D FEM-BEM [10] have been proposed for predicting train-induced ground vibrations. However, most of the existing studies considered the cyclic or moving surface (or point) loads rather than a true train moving loads. The assumption of a cyclic or single wheel moving load rather than true train moving load is highly controversial because the dynamic amplification and critical speed depend on the wavelength of the site and the distance between the axles and bogies of the car [11]. Hence, the actual individual axle load and train geometry need to be considered in the dynamic analysis of the track performance under various conditions of the train-track-ground system, which will be the case in this paper.

In this study, an innovative three-dimensional (3D) finite element (FE) numerical model which was previously established by Sayeed [12] and Sayeed and Shahin [13] was used to investigate the impact of various important parameter that significantly influence the dynamic behavior of ballasted railway track foundation. The parameters considered in this study include the train speed, subgrade thickness, loading amplitude and train geometry. The obtained outcomes were critically analyzed and discussed.

2. Numerical modelling of railway track foundations

In the present study, the dynamic behavior of train-track-ground system was investigated using an advanced 3D FE numerical modelling subjected to train moving load. The finite element based software package GTS-NX [14] was used to develop the 3D railway track model. This software was chosen because of its excellent capability of capturing the true train moving loads at various speeds. In this section, the finite element modelling, and simulations are described briefly.

Finite element model

The three-dimensional FE model developed in the present study is shown in Figure 1. The track dimensions considered were 80 m, 36 m and 15 m in the longitudinal, horizontal and vertical directions, respectively. The rail was modelled using one-dimensional (1D) beam section (I-shaped) running across the railway track length. A UIC-60 section was assumed for the rail, which was fixed to the sleepers by rail pads. The rail pads were characterized by a spring-like elastic link element which stiffness equal to 100 MN/m. The other track components (i.e. sleeper, ballast, subballast and subgrade) were modeled using 3D solid elements. A total of 133 sleepers were placed along the rail at 0.6 m spacing. The rail, sleepers and subgrade were considered as linear elastic (LE) materials, whereas the ballast and subballast were modelled using elastoplastic Mohr-Coulomb (MC) materials. The properties of all materials used in the FE model are summarized in Table 1. It should be noted that the values in Tables 1 are based on similar values given by other researchers [15, 16].

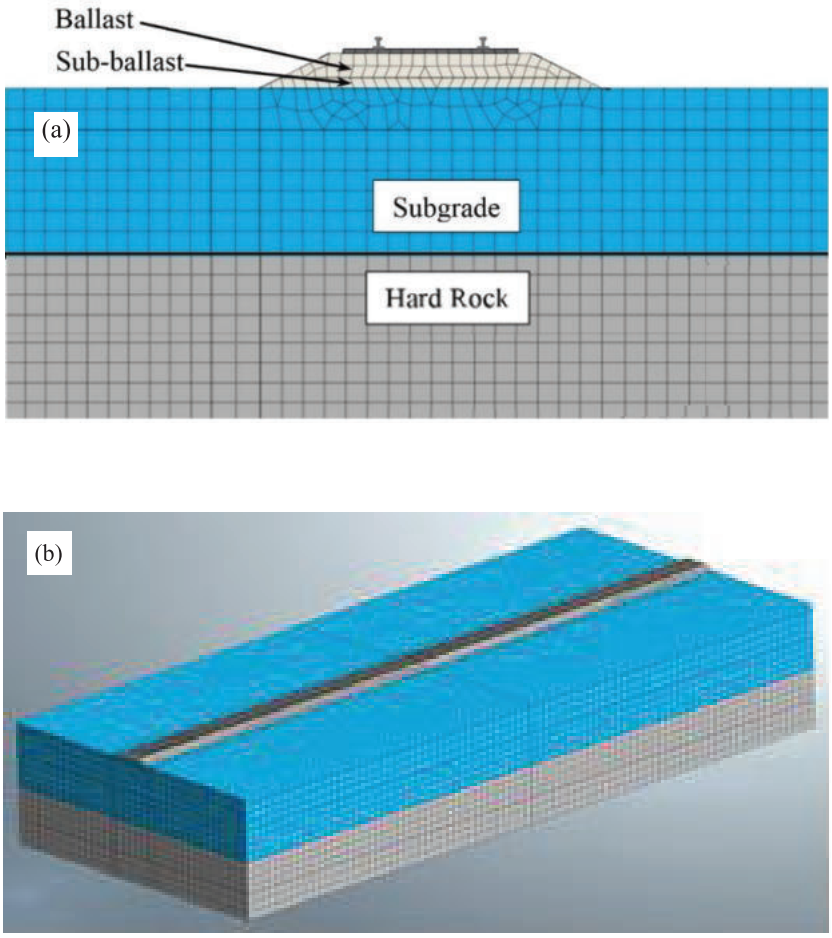

Figure 1. Three-dimensional FE model of railway track-ground system (a) cross-section of the model (not to scale); (b) isometric view of the model.

In the dynamic analyses using finite element model, the size of finite element, time step and model boundaries have to be chosen accurately to ensure the accuracy of results [17]. Generally, the element dimension of the FE numerical model was calculated based on the lowest wavelength which permits the high-frequency wave to be simulated appropriately. Consequently, the dimensions of the 3D finite element model constituents used in this study were chosen as: 0.17 m × 0.14 m × 0.20 m; 0.20 m × 0.20 m × 0.20 m; and 0.60 m × 0.60 m × 0.60 m for the sleepers, ballast and sub-ballast, and subgrade, respectively. Hence, the modelled track FE mesh comprised of 330,000 elements. The viscous dampers were linked to the vertical boundaries of the FE model to absorb the incident compression and secondary waves, and to characterize infinite boundary conditions as suggested by many researchers [18, 19]. To simulate bedrock condition of the track, all nodes at the bottom boundary were set to fix in every direction. The material damping of the model was characterized by Rayleigh damping using the mass and stiffness proportional coefficients that is usually used in the FE dynamic analyses. The general equation of Rayleigh damping is as given below:

$$[C]=\alpha[M]+\beta[K] \tag{1}$$

where, $[C]$ is the damping matrix; $[M]$ and $[K]$ are the mass matrix and stiffness matrix, respectively. The parameters α is the mass proportional damping coefficient and β is the stiffness proportional damping coefficient. These damping coefficients are frequency-dependent and can be calculated using the equations as follows [20]:

$$\alpha = 2\omega_i\omega_j(\xi_i.\omega_j - \xi_j.\omega_i)/(\omega_j{}^2 - \omega_i{}^2) \quad (2)$$

$$\beta = 2(\xi_j.\omega_j - \xi_i.\omega_i)/(\omega_j{}^2 - \omega_i{}^2) \quad (3)$$

where, ω_i and ω_j are the natural frequency of mode-1 and mode-2 of the full model, respectively, for which the effective modal mass participation factors are high in the loading direction; and ξ_i and ξ_j are the hysteretic material damping ratios in the frequency range of interest (see Table 1). It should be noted that the natural frequency mode of the FE model was obtained by an eigenvalue analysis considering the subgrade reaction at the boundary of the layered material mesh using Midas-GTS software.

Table 1. Material properties used in the FE model.

Track component	Material property	Value
Rail	Dynamic modulus of elasticity, E (MPa)	210,000
	Poisson's ratio, v	0.30
	Moment of inertia, I (m^4)	3.04×10^{-5}
Sleeper	Dynamic modulus of elasticity, E (MPa)	30,000
	Poisson's ratio, v	0.20
	Unit weight, γ (kN/m^3)	20.2
	Length, l (m)	2.50
	Width, w (m)	0.27
	Thickness (m)	0.20
Ballast	Dynamic modulus of elasticity, E (MPa)	270
	Poissons ratio, v	0.30
	Unit weight, γ (kN/m^3)	17.3
	Cohesion, c (kPa)	0.00
	Friction Angle, ϕ^o	50.0
	Thickness, H (m)	0.30
	Shear Wave Velocity, C_s (m/s)	243
	Damping Ratio, ξ	0.03
Subballast	Dynamic modulus of elasticity, E (MPa)	135
	Poissons ratio, v	0.35
	Unit weight, γ (kN/m^3)	21.6
	Cohesion, c (kPa)	0.00
	Friction angle, ϕ^o	40.0
	Thickness, H (m)	0.15
	Shear wave Velocity, C_s (m/s)	151
	Damping ratio, ξ	0.03
Subgrade Soil	Dynamic modulus of elasticity, E (MPa)	60.0
	Poissons ratio, v	0.35
	Unit weight, γ (kN/m^3)	18.8
	Thickness, H (m)	7.50
	Shear wave velocity, C_s (m/s)	108
	Raleigh wave velocity, C_R (m/s)	101
	Damping ratio, ξ	0.03

Simulations of train moving load (X-2000 HST)

The standard axle loads, and train geometry used in the FE numerical modelling for the X-2000 HST are summarized in Table 2, which includes (for each car) axle to axle distance (L_a), bogie to bogie distance (L_b), car length (L_c), front wheel load (P_F) and rear wheel load (P_R). A schematic diagram of the X-2000 HST is shown in Figure 2.

In this study, the moving loads of the train were simulated in accordance with Araújo [21]. In this simulation, the finite element rail nodes, which are tightly linked to the sleepers, are subjected to a wheel load (denoted as *loading nodes*) whose value varies over time. As presented in Figure 3, the moving loads can be considered as triangular pulses distributed between three consecutive loading nodes. The wheel load, F, at one specific *loading node*, N+1, raises once the wheel leaves the previous node N, reaches the highest value when the wheel load is directly above the loading node N+1, then finally reducing back to zero when the wheel load reaches the following node N+2. Thus, the triangular pulse moves from one loading node to another by a time interval which is equal to the spacing of the loading nodes divided by the train speed, C, of the moving loads. For example, if the train speed is 60 m/s (216 km/h), the wheel load will pass the distance between two consecutive *loading nodes* (note that the spacing between any two *loading nodes* is 0.6 m) in 0.01 sec. Similarly, a series of train wheels will be moving along the railway track. It should be noted that all FE analyses in the current study were performed in the time domain, which is more natural to reproduce the transient phenomenon of wave propagation [22].

Table 2. Geometry and axle loads of the X-2000 HST Takemiya [23].

Car number, n	Spacing			Standard wheel load	
	L_a (m)	L_b (m)	L_c (m)	P_F	P_R
1	2.9	14.5	22.2	81.0	61.3
2	2.9	17.7	24.4	61.3	61.3
3	2.9	17.7	24.4	61.3	61.3
4	2.9	17.7	24.4	61.3	61.3
5	2.9	9.5	17.2	90.0	90.0

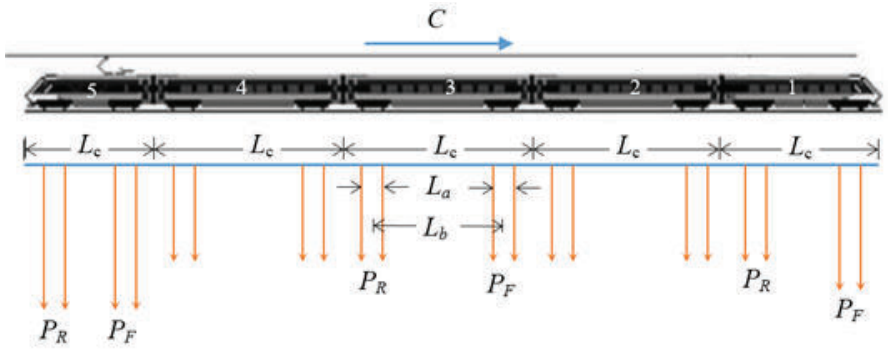

Figure 2. Geometry of the X-2000 HST Takemiya [23].

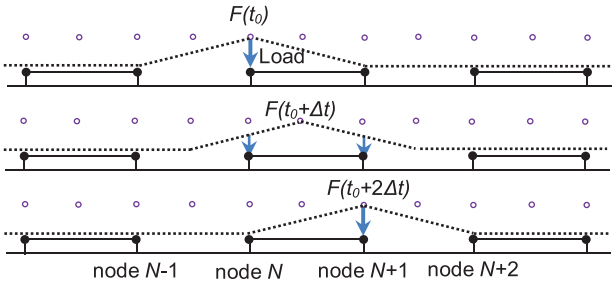

Figure 3. Simulation of moving loads Araújo [21].

3. Results and discussions

In this section, the dynamic responses of the train-track-ground system subjected to train moving loads at different speeds, namely the critical speed, subcritical speed (i.e. speed less than the critical speed), and supercritical speed (i.e.

speed higher than the critical speed) were investigated. As stated earlier, X-2000 HST was considered as the train moving load unless otherwise specified. In addition, various conditions of the train-track-ground system affecting the track performance were examined, including the subgrade thickness, amplitude of train loading and train geometry. The obtained results were critically analyzed and discussed.

Effect of train speed

As stated earlier, train speed is a key factor that effects track behavior. In this section, the influence of train speed was examined for various speeds started from 20 m/s to 290 m/s. The maximum downward and maximum upward displacements of sleeper for each train speed was calculated. Figure 4 shows the track response in terms sleeper displacements versus the train speed. It can be observed that the track response (i.e. sleeper displacement) generally raises with the raise in the train speed. The sleeper displacement reaches its peak value at the critical speed, before it reduces with further raise in the train speed. As can also be seen, the critical speed was found to be higher than both the shear wave (C_s) and Rayleigh wave (C_R) velocities of the top subgrade medium overlying the hard layer of rock. The value of critical speed ≈ 175 m/s, whereas the for the subgrade soil C_s = 114 m/s and C_R = 106 m/s). This result indicates that the critical speed of the train-track-ground system is not always the same to the C_R of the top subgrade soil as occasionally assumed, and this can be related to the presence of the hard rock layer bellow, in which Rayleigh wave velocity is 295 m/s. This behavior shows good reliability in a qualitative sense with the results presented by Alves Costa, et al. [2] and Bian, et al. [10]. Moreover, Figure 4 represents that the impact of train speed on the sleeper downward and upward displacements is negligible when the train speed is less than 30% of the critical speed, and the dynamic influence starts after that train speed. Conversely, the sleeper displacement increases dramatically when the train speed exceeds around 65% of the critical speed and continues the same tendency until it touches the critical speed. Based on the results discussed above, the train speed value up to about 65% of the critical speed may be expected as the safe speed limit for train movement on the train-track-ground system.

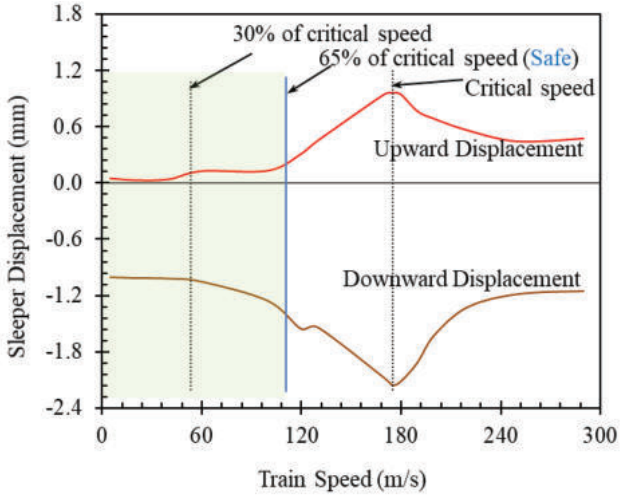

Figure 4. Effect of train speed on sleeper displacement.

Figure 5 shows the time-history sleeper displacement response for three typical speeds, including the subcritical speed (i.e. speed less than the critical speed), critical speed and supercritical speed (i.e. speed higher than the critical speed). The train speed 40 m/s, 175 m/s and 240 m/s were chosen as subcritical, critical and supercritical speed, respectively, from Figure 4. To compare the dynamic behavior of railway track at the specified three train speeds, the sleeper displacements were plotted along a common space axis, transformed from the time axis, t, through multiplication by the speed of train, *C*. It can be observed from Figure 5 that larger sleeper displacements happen at the critical speed (175 m/s) than at the other train speeds (40 m/s and 240 m/s). It can also be noticed that at the subcritical speed (40

m/s), the peaks of sleeper displacements grow at the instant of passage of the individual wheel load for the point under consideration. However, for critical and supercritical speed, the involvement of the four-wheel loads (adjacent two bogies) overlays to give almost one principal peak, and the track oscillates after the train passage. This track response agrees practically well with the earlier simulated response published by Kaynia, et al. [4].

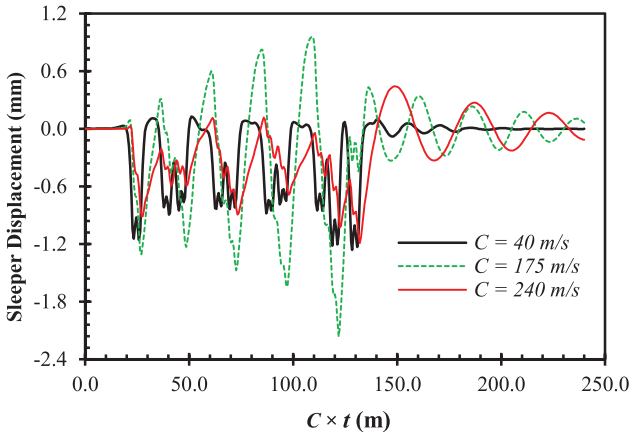

Figure 5. Time-history dynamic response of sleeper displacement for different train speeds.

To illustrate the effect of train speed on the track foundation, the attained vertical deflections along the track (on three-dimensional model) are shown in Figure 6 at the subcritical speed, critical speed and super critical speed. It can be observed from Figure 6(a) that at the subcritical speed (40 m/s), the vertical deflections are primarily occur near the load positions, and there is a small wave propagation to the adjacent ground, as anticipated. In contrast, it can be seen from Figure 6(b) and (c) that at the critical speed of 175 m/s and supercritical speed of 240 m/s, the vertical deflection is not only occurred near the load positions but also in the nearby ground. It can also be observed that a chain of wave fronts emit from the load positions displaying a shockwave in the track ground, which is known as the "Mach cone"; this occurrence is analogous to the incident of sonic boom normally related with supersonic aircraft [24]. These observed results ensure that the FE modelling is reliable and can be used with assurance to estimate the railway track response at any train speeds including the critical and supercritical speed.

Effect of train speed and subgrade thickness

Moreover, the dynamic response of train-track-ground system at different train speed is highly dependent on thicknesses of subgrade [2]. To investigate the impact of the track subgrade thickness on the track performance four different values of the subgrade thickness (i.e. H_s = 5 m, 7.5 m, 10 m and ∞ m) overlying a hard rock were considered. The impact of the train speed and track subgrade thickness is presented in Figure 7, in terms of the relationship between the train speed and sleeper displacement. It can be seen that, for all values of H_s, the downward sleeper displacement increases with the increase of the train speed until it reaches a peak value corresponding to the critical speed, after which it decreases with further increase in the train speed. It can also be seen that the value of critical speed decreases with the increase in the track subgrade thickness. The practical implication of this outcome is there should have a hard rock layer beneath the subgrade soil to increase the critical speed.

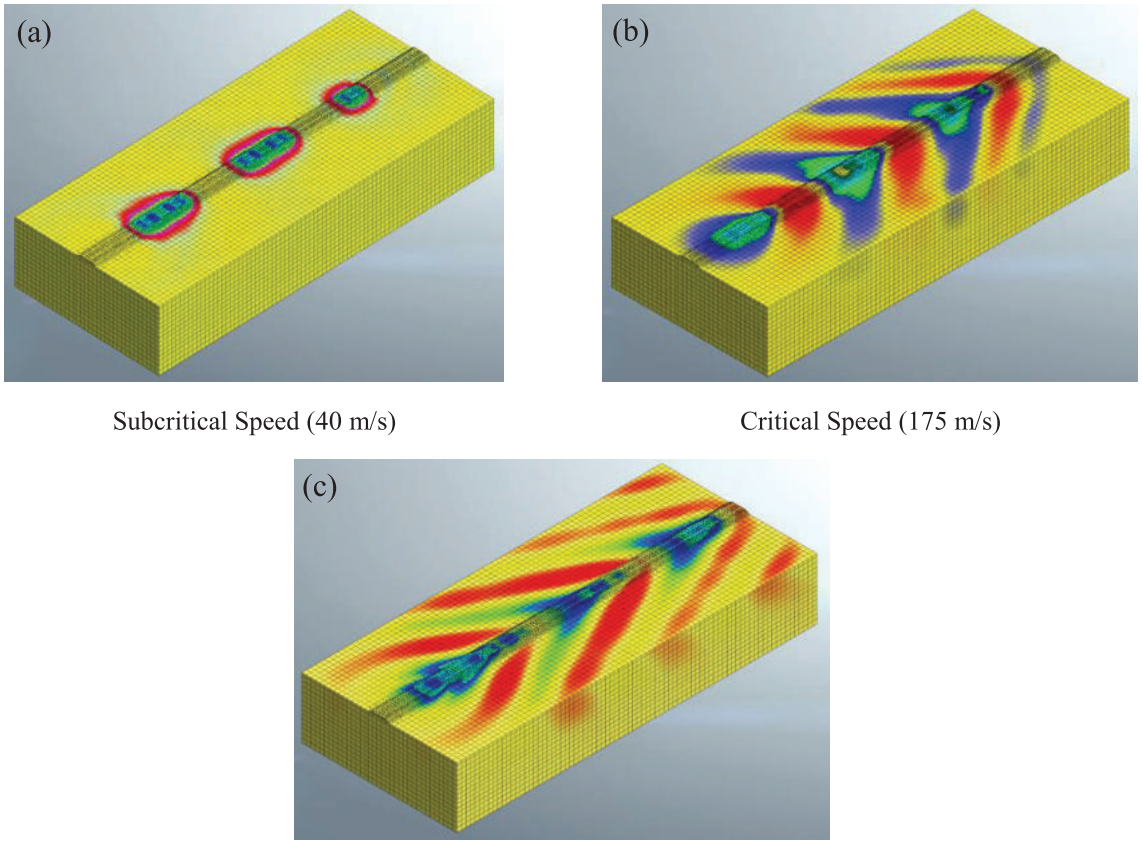

Subcritical Speed (40 m/s)

Critical Speed (175 m/s)

Supercritical Speed (240 m/s)

Figure 6. Typical contour plots of vertical track deflection for: (a) train speed of 40 m/s; (b) train speed of 175 m/s; and (c) train speed of 240 m/s.

Effect of train loading characteristics

In this section, the influence of train loading amplitude and train geometry on the sleeper displacement response was investigated. For this reason, the finite element model for the X-2000 HST with the nominal features given in Table 1 was utilized unless otherwise stated. In order to examine the effect of the amplitude of the train moving loads on the sleeper displacement, six different loading amplitudes (50%, 75%, 100%, 125% and 150%) of the standard X-2000 HST wheel loading were used. The standard wheel loading was considered to be equivalent to the wheel loads that is given in Table 2. The impact of different amplitudes of the wheel loading on the sleeper displacement is shown in Figure 8. It can be seen that the sleeper vertical displacement increases uniformly with the raise of the wheel loading amplitude as one would anticipate.

In the same way, to investigate the effect of the train geometry, six different values of the wheel spacing, L_a were considered in the X-2000 HST. The wheel spacing values were 1.60 m, 1.80 m, 2.20 m, 2.60 m, 3.00 m and 3.40 m. The wheel spacing values chosen herein are based on analogous values stated in the literature [25-27]. The influence of the wheel spacing on the sleeper displacement is shown in Figure 9. It can be seen that the sleeper displacement decreases with the increase in the wheel spacing, as expected.

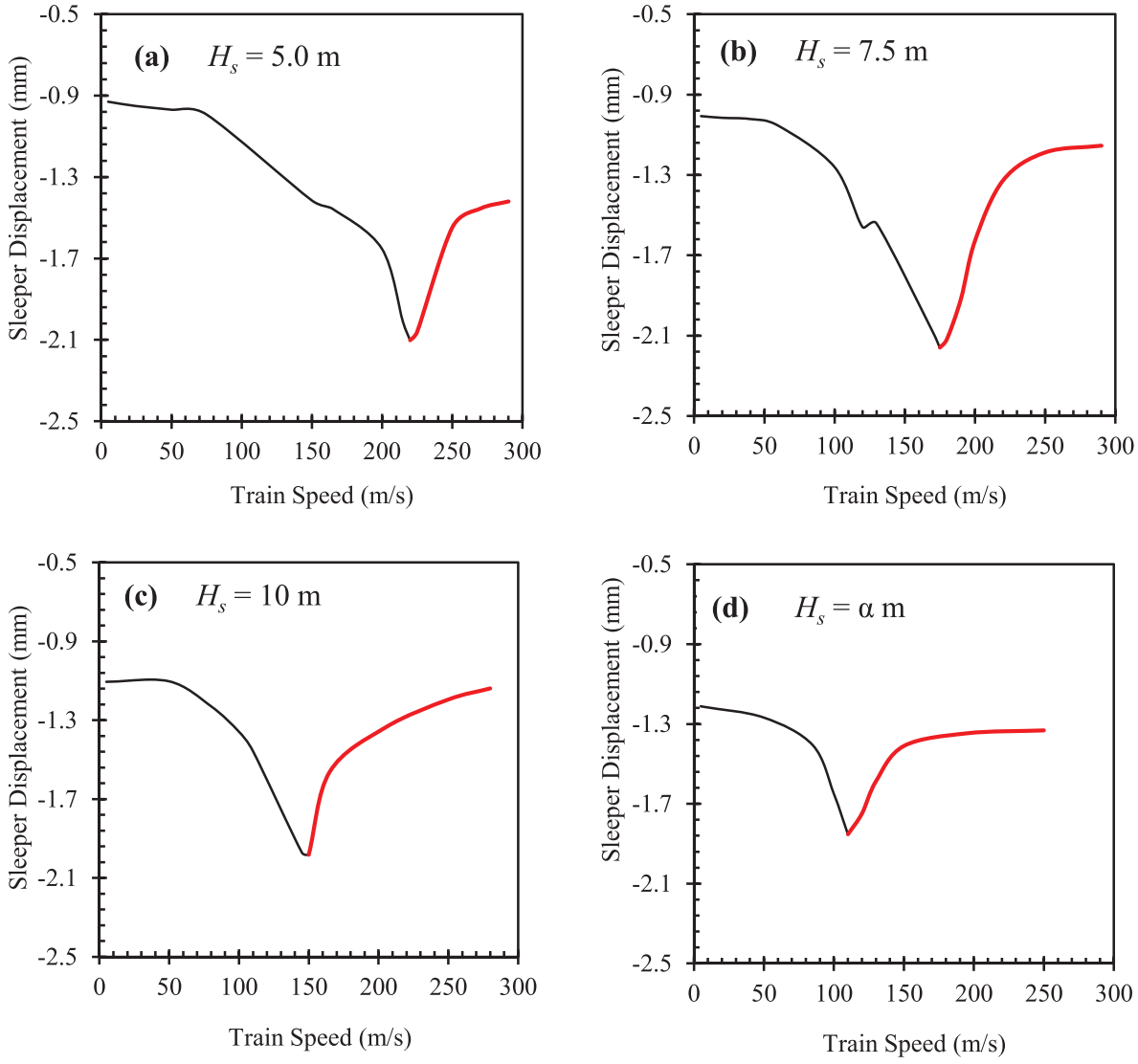

Figure 7. Evolution of sleeper downward deflection versus train speed for different subgrade thicknesses.

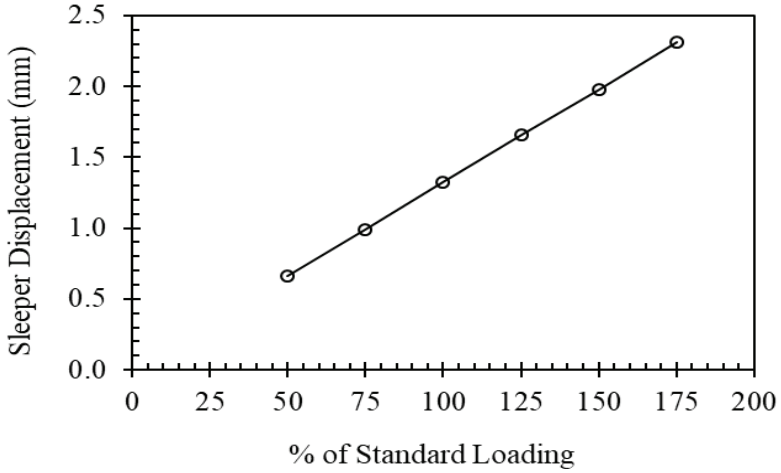

Figure 8. Relationship between track deflection and loading amplitude.

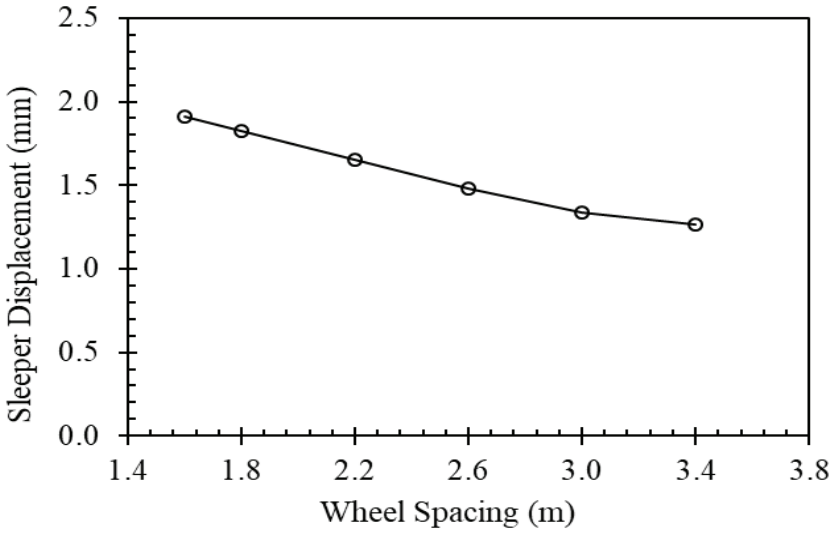

Figure 9. Relationship between track deflection and wheel spacing.

Moreover, to calculate the effect of the wheel spacing so as to be used in a design method a correlation between the wheel spacing and wheel spacing factor (WSF) are established and shown in Figure 10. The WSF is defined as the ratio of the sleeper displacement at particular wheel spacing to the sleeper displacement for the standard wheel spacing of the X-2000 HST. It can be seen that the value of WSF significantly decreases with the increases of the train wheels spacing.

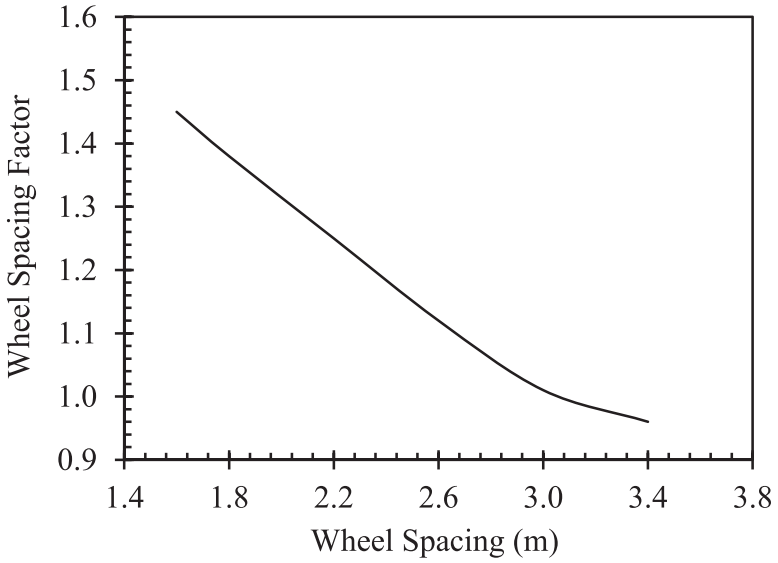

Figure 10. Effect of wheel spacing with respect to standard wheel spacing of the X-2000 HST.

4. Summary and conclusions

In this paper, sophisticated 3D finite elements modelling was performed to simulate the dynamic behavior of ballasted railway track foundation under various conditions of the train-track-ground system including the train speed, subgrade thickness, loading amplitude and wheel spacing. From the obtained results, the following conclusions are drawn:

The amplitude of dynamic track response increases with the increase in the train speed; however, the track response increases rapidly when the train speed exceeds around 65% of the critical speed. Consequently, 65% of the critical speed value can be considered as the acceptable speed limit for safe movement of train.

The subgrade thickness has a significant influence on the track sleeper displacement and critical speed of the train-track-ground system. The value of the critical speed decreases with the increase in the subgrade thickness.
The amplitude of dynamic track response increases uniformly with the amplitude of train loading. On the other hand, the dynamic track response decreases with the increase of wheel spacing.

5. Acknowledgement

The author would like to thank the Department of Civil Engineering and Curtin University for their supports to do this study.

References

[1] V. V. Krylov, A. R. Dawson, M. E. Heelis, and A. C. Collop, "Rail movement and ground waves caused by high-speed trains approaching track-soil critical velocities," *Proceedings of the Institution of Mechanical Engineers, Part F: Journal of Rail and Rapid Transit,* vol. 214, pp. 107-116, 2000.

[2] P. Alves Costa, A. Colaço, R. Calçada, and A. S. Cardoso, "Critical speed of railway tracks. Detailed and simplified approaches," *Transportation Geotechnics,* vol. 2, pp. 30-46, 2015.

[3] C. Madshus and A. M. Kaynia, "High-speed railway lines on soft ground: Dynamic behaviour at critical train speed," *Journal of Sound and Vibration,* vol. 231, pp. 689-701, 2000.

[4] A. M. Kaynia, C. Madshus, and P. Zackrisson, "Ground vibration from high-speed trains: Prediction and countermeasure," *Journal of Geotechnical and Geoenvironmental Engineering,* vol. 126, pp. 531-537, 2000.

[5] H. A. Dieterman and A. V. Metrikine, "Steady-state displacements of a beam on an elastic half-space due to a uniformly moving constant load," *European Journal of Mechanics, A/Solids,* vol. 16, pp. 295-306, 1997.

[6] X. Sheng, C. J. C. Jones, and D. J. Thompson, "A theoretical study on the influence of the track on train-induced ground vibration," *Journal of Sound and Vibration,* vol. 272, pp. 909-936, 2004.

[7] A. El Kacimi, P. K. Woodward, O. Laghrouche, and G. Medero, "Time domain 3D finite element modelling of train-induced vibration at high speed," *Computers and Structures,* vol. 118, pp. 66-73, 2013.

[8] L. S. Sowmiyaa, J. T. Shahu, and K. K. Guptac, "Effect of geosynthetic reinforcement on clayey subgrade – three dimensional finite element analysis on railway track," in *Procedings of the International Conference on Ground Improvement and Ground control*, 2012.

[9] L. Andersen and S. R. Nielsen, "Boundary element analysis of the steady-state response of an elastic half-space to a moving force on its surface," *Engineering Analysis with Boundary Elements,* vol. 27, pp. 23-38, 2003.

[10] X. Bian, C. Cheng, J. Jiang, R. Chen, and Y. Chen, "Numerical analysis of soil vibrations due to trains moving at critical speed," *Acta Geotechnica,* vol. 11(2), pp. 1-14, 2014.

[11] M. A. Sayeed and M. A. Shahin, "Investigation into Impact of Train Speed for Behavior of Ballasted Railway Track Foundations," *ICTG*, *Procedia Engineering,* vol. 143, pp. 1152-1159, 2016.

[12] M. A. Sayeed, "Design of ballasted railway track foundations using numerical modelling with special reference to high speed trains," *PhD Thesis*, Curtin University, 2016.

[13] M. A. Sayeed and M. A. Shahin, "Three-dimensional numerical modelling of ballasted railway track foundations for high-speed trains with special reference to critical speed," *Transportation Geotechnics,* vol. 6, pp. 55-65, 2016.

[14] MIDAS IT. Co. Ltd., *Manual of GTS-NX 2013 v1.2: New experience of geotechnical analysis system*, MIDAS Company Limited, South Korea 2013.

[15] E. T. Selig and D. Li, "Track modulus: Its meaning and factor influencing it," *Transportation Research Record,* vol. 1470, pp. 47 - 54, 1994.

[16] J. T. Shahu, N. S. V. Kameswara Rao, and Yudhbir, "Parametric study of resilient response of tracks with a sub-ballast layer," *Canadian Geotechnical Journal,* vol. 36, pp. 1137-1150, 1999.

[17] V. Galavi and R. B. J. Brinkgreve, "Finite element modelling of geotechnical structures subjected to moving loads," in *VIII ECNUMGE - Numerical Methods in Geotechnical Engineering*. vol. 1, Hicks et al., Netherlands, Taylor and Francis - Balkema, pp. 235-240, 2014.

[18] G. Kouroussis, O. Verlinden, and C. Conti, "Finite-dynamic model for infinite media: Corrected solution of viscous boundary efficiency," *Journal of Engineering Mechanics,* vol. 137, pp. 509-511, 2011.

[19] J. Lysmer and R. L. Kuhlemeyer, "Finite dynamic model for infinite media," *Journal of the Engineering Mechanics Division, ASCE,* vol. 95, pp. 859-877, 1969.

[20] I. Chowdhury and S. P. Dasgupta, "Computation of Rayleigh damping coefficients for large systems," *The Electronic Journal of Geotechnical Engineering,* vol. 8, pp. 1-11, 2003.
[21] N. M. F. Araújo, "High-speed trains on ballasted railway track: Dynamic stress field analysis," *PhD Thesis, Universidade do Minho, Portugal*, 2011.
[22] G. Kouroussis, O. Verlinden, and C. Conti, "Ground propagation of vibrations from railway vehicles using a finite/infinite-element model of the soil," *Journal of Rail and Rapid Transit,* vol. 223, pp. 405-413, 2009.
[23] H. Takemiya, "Simulation of track-ground vibrations due to a high-speed train: the case of X-2000 at Ledsgard," *Journal of Sound and Vibration,* vol. 261, pp. 503-526, 2003.
[24] V. V. Krylov, *Noise and Vibration from High-speed Trains*, London, Thomas Telford, 2001.
[25] T. Jeffs and G. P. Tew, *A review of track design procedures, Vol. 2, Sleepers and Ballast*, BHP Research - Melbourne Laboratories, Railways of Australia, Victoria, Australia, 1991.
[26] G. Kouroussis, O. Verlinden, and C. Conti, "Free field vibrations caused by high-speed lines: measurement and time domain simulation," *Soil Dynamics and Earthquake Engineering,* vol. 31, pp. 692-707, 2011.
[27] L. Hall, "Simulations and analyses of train-induced ground vibrations in finite element models," *Soil Dynamics and Earthquake Engineering,* vol. 23, pp. 403-413, 2003.